55

Journal of the Meteorological Society of Japan, Vol. 74, No. 6, pp. 909–921, 1996

Time Spectral Analysis for the Natural Variability of the Barotropic Model Atmosphere with Annual Cycle Forcing

By H.L. Tanaka, Kazuo Kimura[1] and Tetsuzo Yasunari

Institute of Geoscience, University of Tsukuba, Tsukuba, 305 Japan

(Manuscript received 2 May 1996, in revised form 14 October 1996)

Abstract

In this study, a long-term (1000 years) integration of a simple barotropic primitive equation model was carried out to investigate the typical magnitude and spectral features of natural variability of the model atmosphere.

The first experiment without an annual-cycle forcing shows no noticeable ultra-low-frequency variability. The frequency spectrum of the model atmosphere is characterized as a white noise for the low-frequency range beyond the period about 50 days. The spectrum then shifts sharply to a red noise for the period shorter than 50 days, indicating a characteristic -3 power slope over the frequency domain. Although no noticeable spectral peak is detected, we can find intraseasonal variability with a period of about 50 days in the time series of the model atmosphere as a result from the sharp transition from the red to white noise. Since the sole energy source of the system is a parameterized baroclinic instability of frequency about $(5\text{-day})^{-1}$, we must have a reverse energy cascade from higher- to lower-frequency ranges along the -3 power slope of the red noise spectrum. It is discussed in this study that the spectrum tends to be red over the high-frequency range beyond $(50\text{-day})^{-1}$ where a linear relation holds between life-time and spatial scales for prominent atmospheric phenomena. Beyond this period, the internal non-linear dynamics of the primitive equation can not sustain large energy because the spatial scale of the Earth is finite. As a result, the very-low-frequency variability results in the white noise spectrum.

Next, the same simple model is integrated with an annual-cycle forcing for 100 years to investigate the excitation of harmonics and subharmonics expected by the non-linear dynamic modulation of the annual-cycle forcing. The results show, however, that the spectral features are not altered by the inclusion of the annual cycle, except for the isolated spectral peak associated with the annual-cycle forcing. We suggest from the results of this study that the harmonics and subharmonics, such as semiannual and biennial oscillations, are not excited solely by the non-linear dynamic modulation of the forced annual cycle in the atmosphere.

1. Introduction

Low-frequency variability in nature may be classified in two components: one is caused by external forcing and the other by internal natural variability which occurs even under a fixed boundary condition. A detailed analysis of the low-frequency variability and ultra-low-frequency variability is an important research subject in the issues of long-range forecasting and the global change. The first step to assess the low-frequency variability is to separate the natural variability of the atmosphere from the forced trend and variability due to external forcing such as El-Niño events, volcanic eruptions, and increased anthropogenic greenhouse gases. However, little is known about the nature, magnitude, or the spectral features of the internally-generated low-frequency variability.

Atmospheric general circulation models under a fixed boundary condition or a prescribed sea surface temperature (SST) indicate their own natural variability determined by the characteristic physical processes included in the models (see Hansen *et al.*, 1988; Sperber and Palmer, 1995). Likewise, coupled atmosphere-ocean models and more complicated climate system models would indicate their own natural variability under a wider class of fixed boundary conditions, such as the type of gas constituent

1 Present Affiliation: Hamagin Research Institute, Ltd. Yokohama, 220 Japan.

and astronomical parameters (*e.g.*, Stouffer *et al.*, 1989; 1994; Wigley and Raper, 1990; Manabe *et al.*, 1991; Manabe and Stouffer, 1996). With an energy-balance model, Wigley and Raper (1990) showed that a simple ocean model can produce a natural trend of up to 0.3°C during 100 years solely by the internal natural variability of the model. The process which determines the magnitude of the natural variability depends highly on the complexity of the model. However, it is not clear to what extent the natural variability depends on the complexity and the internal non-linear structure of the model. Even a simple baroclinic model with an energy source and sink (*e.g.*, James and Gray, 1986; James and James, 1989; James *et al.*, 1994) can show its characteristic natural variability. Hence, it is an interesting subject to evaluate the magnitude of the natural variability for different climate models and find some rules between the model complexity and the induced natural variability.

Recently, a new type of a simple barotropic model with an energy source and sink was developed by Tanaka (1991) based on a three-dimensional normal mode expansion of the atmospheric variables. The model is capable to simulate a realistic low-frequency variability, such as blocking events on a sphere, and is sufficiently fast to integrate in time. Therefore, it is straightforward to apply the model for a study of natural variability of a simple model atmosphere. The first objective of this study is to find the characteristics and typical magnitude of the natural variability of the model atmosphere by a long-term (1000 years) integration of the simple model under a fixed boundary condition. The results will be compared with the natural variability of other simple models (*e.g.*, James and James, 1989; James *et al.*, 1994).

The next step of this study is to introduce the fundamental atmospheric periodicity of the annual cycle. James and James (1989) reported that the interannual variability with periods of up to 10–40 years was generated internally by the non-linear dynamics of a simple primitive equation model with an imposed annual-cycle forcing. According to the recent study by Zhao and Takahashi (1996), intraseasonal and interannual oscillations may be excited by superharmonic and subharmonic resonances of the seasonal cycle, respectively. Zhao and Takahashi considered the response of the tropical Kelvin waves to the cumulus heating with a seasonal cycle under a certain form of damping to derive the so-called Mathieu equation. The Mathieu equation is linear with respect to a state variable and is regarded as a simple harmonic oscillator with an external annual forcing which is, however, a function of the state variable. The solution is known to have superharmonic and subharmonic resonances, that is referred to as parametric instability, induced by the annual forcing. It is our aim to investigate the parametric instability under a fully non-linear primitive equation model.

The main objective of this study is to find if the imposed annual-cycle forcing could generate its harmonics and subharmonics over the rest of the frequency domain. Semiannual and biennial oscillations or the intraseasonal and interannual variabilities might be excited as the non-linear modulation of the strong annual cycle. The results will be compared with the aforementioned 1000-year run without the annual forcing to assess the role of the forced annual cycle on the low-frequency natural variabilities.

A brief description of the spectral primitive equation model is given in Section 2. The results for a 1000-year run without the annual-cycle forcing is presented in Section 3. In Section 4, we describe the results for a 100-year run with the annual-cycle forcing. Section 5 is devoted to a summary of our results and some concluding remarks.

2. Model description

The model description is detailed in Tanaka (1991), and a brief description is presented here. A system of primitive equations with a spherical coordinate of longitude λ, latitude θ, pressure p, and time t may be reduced to three prognostic equations of horizontal motions and thermodynamics for three dependent variables of $U=(u, v, \phi)^T$. Here, u and v are the zonal and meridional components of the horizontal velocity. The variable ϕ is a departure of the local isobaric geopotential from the global mean reference state, and the superscript T denotes a transpose. Using a matrix notation, these primitive equations may be written as

$$M\frac{\partial U}{\partial t} + LU = N + F. \tag{1}$$

The left-hand side of (1) represents linear terms with matrix operators M and L and the dependent variable vector U. The right-hand side represents a non-linear term vector N and a diabatic term vector F which includes the zonal and meridional components of frictional forces and a diabatic heating rate.

In order to obtain a system of spectral primitive equations, we expand the vectors U and F in 3-D normal mode functions in a resting atmosphere, $\Pi_{nlm}(\lambda, \theta, p)$:

$$U(\lambda,\theta,p,t) = \sum_{n=-N}^{N}\sum_{l=0}^{L}\sum_{m=0}^{M} w_{nlm}(t)X_m\Pi_{nlm}(\lambda,\theta,p), \tag{2}$$

$$F(\lambda,\theta,p,t) = \sum_{n=-N}^{N}\sum_{l=0}^{L}\sum_{m=0}^{M} f_{nlm}(t)Y_m\Pi_{nlm}(\lambda,\theta,p). \tag{3}$$

Here the expansion coefficients $w_{nlm}(t)$ and $f_{nlm}(t)$ are the functions of time alone. The subscripts represent zonal wavenumbers n, meridional indices l, and vertical indices m. They are truncated at N, L, and M, respectively. The model truncation is extended in this study to zonal wavenumber 20, which is comparable to rhomboidal 20 truncation with an equatorial wall. The scaling matrices X_m and Y_m should be defined for each vertical index. The 3-D normal mode functions $\Pi_{nlm}(\lambda, \theta, p)$ are given by a tensor product of vertical structure functions (vertical normal modes) and Hough harmonics (horizontal normal modes) associated with the linear operators M and L, respectively. It is known that they form a complete set and satisfy an orthonormality condition under a proper inner product $\langle\ ,\ \rangle$ as:

$$\langle \Pi_{nlm}, \Pi_{n'l'm'} \rangle = \delta_{nn'}\delta_{ll'}\delta_{mm'}, \tag{4}$$

where the symbols δ_{ij} is the Kronecker delta.

Applied to the inner product for (1), the weak form of primitive equation becomes

$$\left\langle M\frac{\partial U}{\partial t} + LU - N - F, Y_m^{-1}\Pi_{nlm} \right\rangle = 0. \tag{5}$$

Substituting (2) and (3) into (5), rearranging the time-dependent variables, and evaluating the remaining terms, we obtain a system of 3-D spectral primitive equations in terms of the spectral expansion coefficients:

$$\frac{dw_i}{d\tau} + i\sigma_i w_i = -i\sum_{jk} r_{ijk} w_j w_k + f_i, \quad i = 1, 2, 3, \ldots \tag{6}$$

where τ is a dimensionless time, the symbol σ_i denotes the eigenfrequency of the normal mode at a resting atmosphere, and r_{ijk} is the interaction coefficient for non-linear wave-wave interactions. For simplicity, the triple subscripts nml are shortened to a single subscript i.

The spectral primitive Eq. (6) is integrated by Tanaka (1995) for the study of a life-cycle of nonlinear baroclinic waves. The result clearly shows that baroclinic waves draw energy from baroclinic components of the atmosphere and feed the energy to the barotropic components. It was found that the important baroclinic-barotropic interaction is accomplished by baroclinic instability, which pumps the zonal baroclinic energy to barotropic components of the atmosphere.

The process of baroclinic instability may be readily analyzed by linearizing (6) with respect to a proper zonal basic state. In order to solve the most unstable linear mode, a perturbation method is introduced using notations $\overline{w}_i$ for a time-independent zonal basic state and w' for small perturbations superimposed on the basic states (the same symbols with the original variables are used for convenience). The equation for the first-order term of perturbations becomes

$$\frac{dw_i}{d\tau} + i\sigma_i w_i = -i\sum_{j=1}^{K}\left(\sum_{k=1}^{K}(r_{ijk} + r_{ikj})\overline{w}_k\right)w_j, \quad i = 1, 2, 3, \ldots, \tag{7}$$

where the index k is used for the basic state and i and j for the perturbations. Here, inviscid and adiabatic eddy is examined, disregarding the perturbations of forcing. For a zonal basic state ($\overline{w}_k \neq 0$ if $n=0$), we can rewrite the equation in terms of a matrix form for each $n \geq 0$:

$$\frac{d}{d\tau}W_n + iD_nW_n = -iB_nW_n, \quad n = 1, 2, \ldots, N, \tag{8}$$

where

$$W_n = (w_1, \ldots w_i, \ldots w_K)^T, \tag{9}$$

$$D = diag(\sigma_1, \ldots \sigma_i, \ldots \sigma_K), \tag{10}$$

and $K = (L+1)(M+1)$. The (i, j) entries of the matrices B, namely b_{ij}, are evaluated by the expansion coefficients of the basic state $\overline{w}_k$:

$$b_{ij} = \sum_{k=1}^{K}(r_{ijk} + r_{ikj})\overline{w}_k, \quad i, j = 1, 2, \ldots, K, \tag{11}$$

The zonal-wave interaction B_n vanishes for a basic state at rest ($\overline{w}_k = 0$), thus the Eq. (8) satisfies the normal mode relation for Laplace's classical tidal theory.

Because (8) is linear, we can assume the solution of W_n as:

$$W_n(\tau) = \xi \exp(-i\nu\tau). \tag{12}$$

The initial value problem (8) is then reduced to an eigenvalue problem for a real matrix to obtain eigenvectors ξ and eigenvalues ν as:

$$\nu\xi = (D_n + B_n)\xi. \tag{13}$$

Those eigenpairs ν and ξ are evaluated by the standard matrix eigenvalue solver. They will be used as the important tools of the parameterization of baroclinic instability for a barotropic model. The distribution of the growth rates and the structure of the unstable modes are discussed by Tanaka and Kung (1989) and Tanaka and Sun (1990) for a basic state of monthly mean FGGE (First GARP Global Experiment) data for January 1979. The growth rate of the most unstable Charney mode is about 0.47 day^{-1} at the zonal wavenumber 7, which corresponds to an e-folding time about 2 days.

In the 3-D spectral representation, the vertical expansion basis functions may be divided into barotropic and baroclinic components. In this study,

we attempt to construct a spectral barotropic model, using only the barotropic components (m=0) of w_i. The spectral equations for such a barotropic model have the same form as for the baroclinic model (6), except the fact that the barotropic-baroclinic interactions should be included formally in f_i. In this study, we consider the following physical processes:

$$f_i = (BC)_i + (DF)_i + (DZ)_i + (DP)_i, \qquad (14)$$

where $(BC)_i$ represents the baroclinic instability, $(DF)_i$ the biharmonic diffusion, $(DZ)_i$ the zonal surface stress, and $(DP)_i$ the damping of planetary waves. The unique energy source of the model is $(BC)_i$ as a major part of the barotropic-baroclinic interactions, and the rest of the three physical processes are the energy sinks of this model.

The baroclinic instability is parameterized using a complex eigenvector ξ_i obtained as an eigenvalue problem (13):

$$\begin{aligned}(BC)_i &= -i\nu(\tau)a(\tau)\xi_i,\\ a(\tau) &= (\xi_i, w_i),\end{aligned} \qquad (15)$$

where the operator $(\,,)$ is a vector inner product of complex numbers, which evaluates the orthogonal projection of w_i onto the unstable subspace ξ_i for each zonal wavenumber. The growth rate of the most unstable mode $\nu(\tau)$ associated with ξ_i is treated as constant ν_0 for the 1000-year integration in Section 4. In Section 5, $\nu(\tau)$ is consider to vary with a one-year period. Since $(BC)_i$ is the unique energy source of the model, changing the growth rate may be the simplest way to introduce an annual oscillation:

$$\nu(\tau) = \left(0.8 + 0.2\cos\left(\frac{2\pi\tau}{T}\right)\right)\nu_0. \qquad (16)$$

The growth rate ν_0 is evaluated for a northern winter basic state by Tanaka and Kung (1989). According to the computation, the peak value of the growth rate of Charney modes (0.47 day^{-1}) for a winter basic state is reduced to about 60 % (0.27 day^{-1}) for a summer basic state. For this reason, the growth rate is controlled in this study to oscillate at a one-year period T within the 60–100 % range of ν_0. As will be shown in the results, the annual cycle so introduced by this variation results in a quite reasonable range of the annual cycle of total energy, in comparison with the observational analyses by Kung (1988) and Tanaka and Kung (1988).

When the model is integrated in time, the energy of smaller-scale eddies is transferred to planetary waves by the up-scale energy cascade as the features of the two-dimensional turbulent flow. Without the assistance of a damping mechanism, the energy is accumulated excessively in planetary waves, and they start to propagate westward in the model atmosphere. In this study, we imposed a small damping for planetary waves to stop such a westward propagation. The damping is applied only to the highest-frequency (*i.e.*, the largest σ_i) planetary waves which are supposed to propagate westward under the scale argument by Dickinson (1968). The magnitude of the damping is assumed to be proportional to the vertical group velocity, evaluated as $\frac{\partial\sigma_i}{\partial h}$:

$$(DP)_i = -\beta\frac{\partial\sigma_i}{\partial h}w_i, \qquad (17)$$

where h is an equivalent height and β is an appropriate damping constant.

In present study, we analyzed the time series of total energy (*i.e.*, sum of kinetic energy and available potential energy) as one of the most fundamental variables representing the global state of the atmosphere. In the spectral domain, the total energy is simply the sum of the energy elements E_{nlm} which is defined by the squared magnitude of the state variables w_{nlm}:

$$E_{nlm} = \frac{1}{2}p_s h_m |w_{nlm}|^2, \qquad (18)$$

where p_s is surface pressure of the reference state. It is not necessary to transform all state variables to the physical space from the spectral space. The choice of total energy for the time series analysis is rather arbitrary but is the most suitable variable for an analysis of extremely long time series, such as 1000-year runs.

3. Results of a control run without an annual cycle

We integrated the simple barotropic model for 1000 years as a control run under a fixed boundary condition. Figure 1 illustrates the time series of the total energy of the model atmosphere for 1, 10, 100, and 1000 years, respectively for (a) to (d). The model output is stored every 24 hours. These time series are the plots of daily values and 10-day, 100-day, and 1000-day averages, respectively. Namely, every panel of the time series contains 365 points of data.

Figure 1a shows a smooth variation of the energy level, starting from about 11 × 10^5 Jm^{-2}. The energy has increased to 17 × 10^5 Jm^{-2} after about 20 days and has reached to a level of equilibrium, fluctuating around the mean. This time series seems to contain a low-frequency variability with a period of approximately 50 days. Figure 1b illustrates a similar time series, but for 10-day mean values during 10 years. We can see the initial increase at the first 20 days at the left-most edge of the time series. The energy level varies within a range from 14 to 22 × 10^5 Jm^{-2}. This range characterizes the magnitude of the natural variability of the model atmosphere. Figure 1c is for the 100-day mean time series during

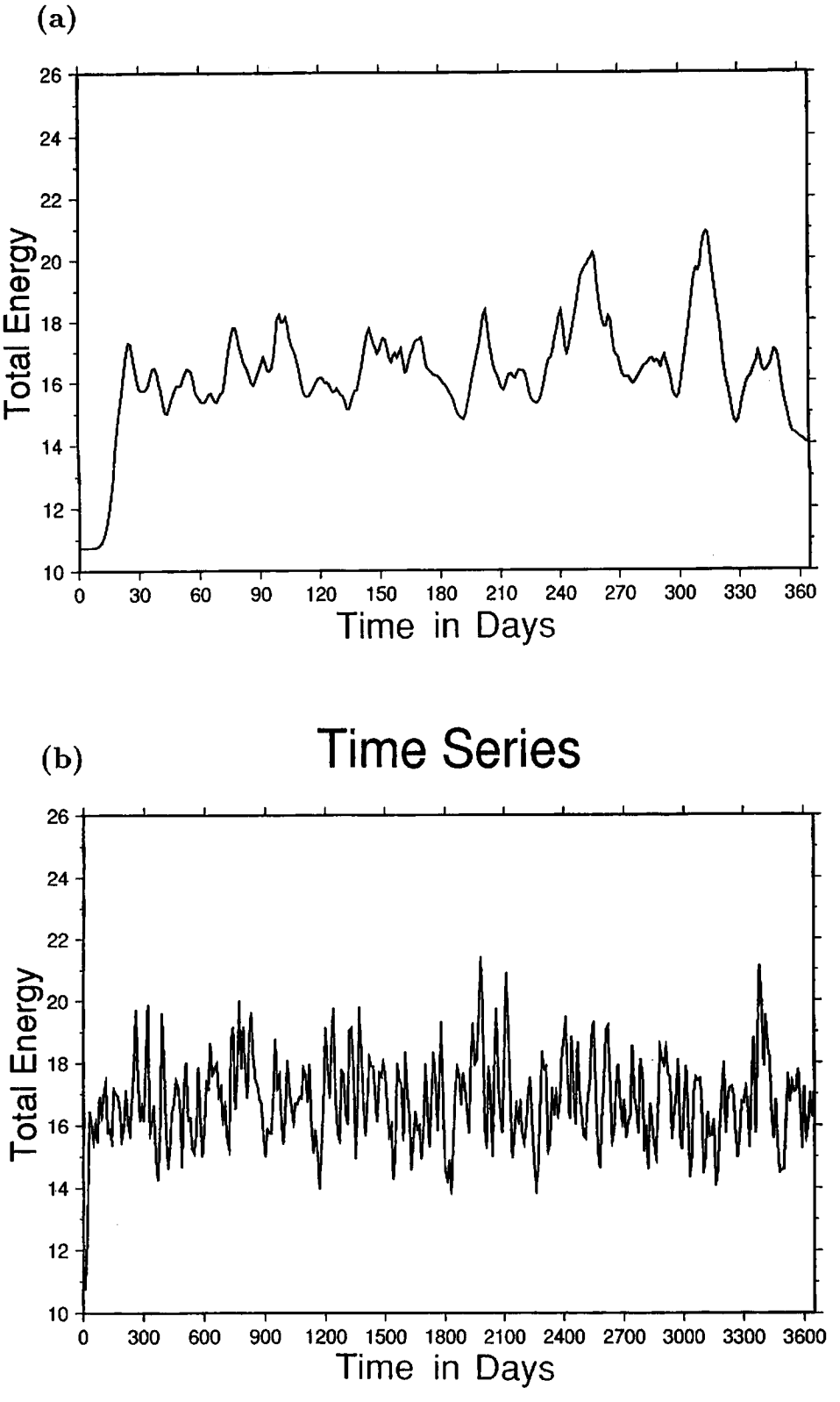

Fig. 1. Time series of the total energy of the control run for 1, 10, 100, and 1000 years, respectively for (a) to (d). The values in the figures contain 365 points of daily value, 10-day mean, 100-day mean, and 1000-day mean, respectively for (a) to (d). The units are 10^5 Jm^{-2}.

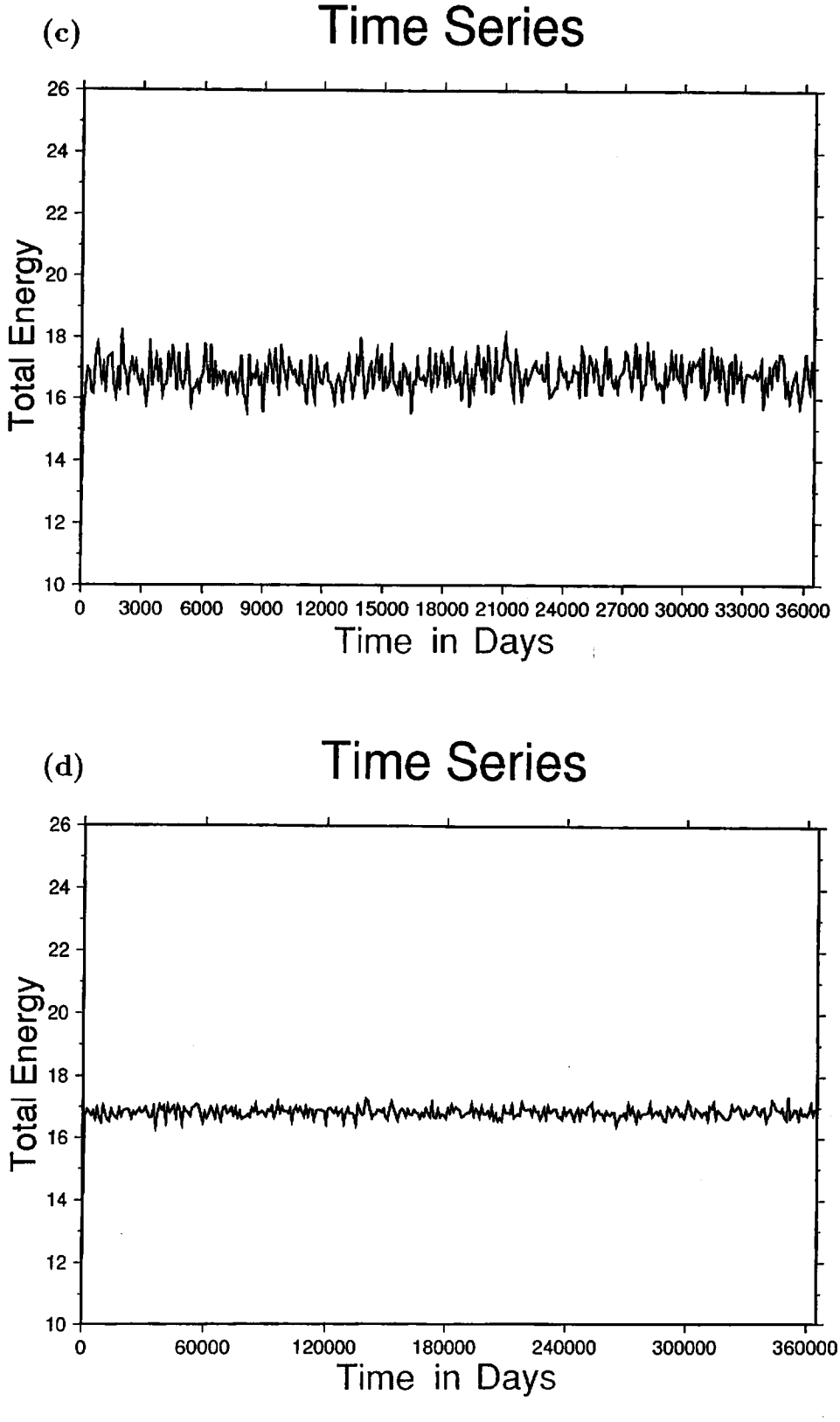

Fig. 1. (Continued)

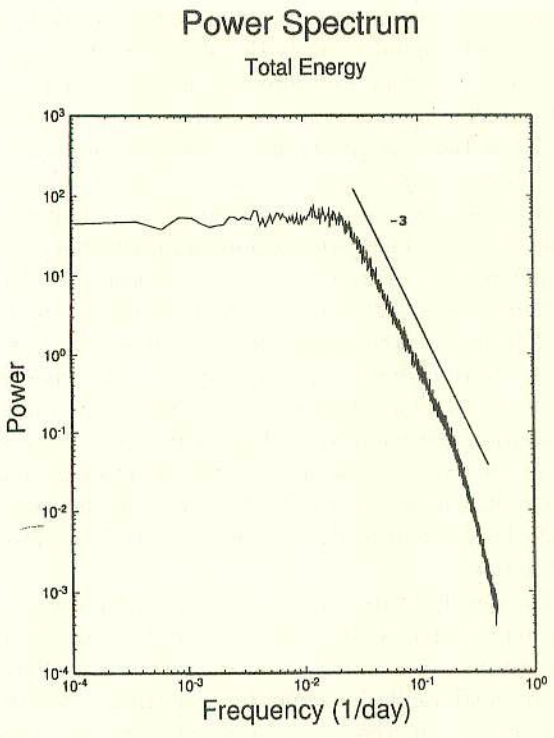

Fig. 2. Power spectrum of the time series of the total energy for the 1000-year integration. The power spectrum is estimated by the FFT routines and is smoothed by averaging 64 terms of the original power spectrum.

100 years. Since the 100-day mean filters out most of the dominant internal fluctuations, the range of the natural variability is reduced substantially compared with the 10-day mean time series in Fig. 1b. Finally, Fig. 1d illustrates the 1000-day mean time series during 1000 years. The range of the natural variability has been reduced to about 1×10^5 Jm^{-2} for this time scale. This time series differs substantially from that of Fig. 1a in its characteristics of variation. It is found by this demonstration that there is practically no ultra-low-frequency variability at this time scale.

Figure 2 illustrates the power spectrum of the time series of the total energy for the 1000-year integration. The power spectrum is estimated by the standard FFT routines with the 1000-year daily data. Since the frequency resolution is so fine, the original power spectrum is averaged for every 64 terms over the frequency domain to plot the smoothed spectrum. The frequency resolution of the spectrum is still fine enough to argue the detailed spectral properties.

The result clearly separates the two characteristic spectral slopes at the low- and high-frequency ranges. Obviously, the spectrum is white for the period beyond 50 days. In other words, the random variable has no memory of the past for a variation beyond the 50-day period. In contrast, the spectrum is red for periods shorter than 50 days. Namely, the random variable remembers its own past to some extent for a variation of periods shorter than 50 days. Interestingly, the spectral slope for the red noise obeys approximately the -3 power of the frequency. The model has an energy source of frequency near (5-day)$^{-1}$ due to the parameterized baroclinic instability. Separated by this energy source, the spectral slope shifts to -4 power of the higher-frequency range over (5-day)$^{-1}$ to (2-day)$^{-1}$. The red-noise spectrum extends over the range up to (50-day)$^{-1}$. Although there is no apparent spectral peak near (50-day)$^{-1}$, we can observe a dominant variation of time scale about 50 days, as in Fig. 1a, due to the fact of the dominant spectral power at this range relative to the higher frequency range of the red noise.

According to Wigley and Raper (1990), a simple energy balance model for global mean temperature changes may be reduced to a simple statistical-dynamical model described by Hasselmann (1976) in a form:

$$\frac{d\Delta T}{dt} = -\lambda \Delta T + \Delta Q, \tag{19}$$

where ΔT is changes of the global mean ocean temperature, ΔQ is a heating rate which is considered as white-noise forcing with a uniform spectrum, and λ is a feedback parameter. The linear term in the right-hand side stands for the thermal inertia of the thermodynamic system represented by the feedback parameter λ, and the white-noise forcing describes high-frequency fluctuations induced by the atmospheric weather system. As the analytical solution of the system, the frequency spectrum becomes white at very-low-frequencies due to the predominant white-noise forcing compared with the linear term on the right-hand side. In contrast, the temperature response to a white-noise forcing produces a red-noise frequency spectrum with a slope of -2 power at the high-frequency range due to the thermal inertia of the ocean. There is a clear transition from the white-noise to red-noise spectra. The spectral features agree well with the present study, although the slope of the red noise is slightly different.

With a multi-level primitive-equation model (run B), James *et al.* (1994) obtained a frequency spectrum of approximately -3 power slope at the high-frequency range and an abrupt transition to white-noise spectrum at the low-frequency range, as obtained in the present study. The transition occurs at the frequency corresponding to about a 60-day period. In their study, the time series investigated is not the total energy but the first principal component of the zonal jet which represents a global characteristic of the model atmosphere. Their model has 5 vertical levels, but a seven-folding symmetry (n=0, 7, 14) is imposed for T21 truncation. Hence, the

degree of freedom of their model is comparable to our model. The power spectrum obtained by James *et al.* (1994) contains more variability at the low-frequency range than the present result. The difference comes mainly from the variability in zonal motions which are relaxed to the climate value in this study by $(DZ)_i$. The overall spectral features in Fig. 2 are thus determined by zonal eddies in the present model.

We may infer from this demonstration that the non-linear dynamics of the primitive equation model produces a pure white-noise spectrum at the ultra-low-frequency range. The contribution from the non-linear advection term may be treated as a white-noise forcing for the low-frequency range. Some linear terms tend to dominate the white-noise forcing at the high-frequency range beyond $(50\text{-day})^{-1}$ where a red-noise spectrum is created out of the transient forcing. It is not clear, however, why the red-noise slope for the non-linear primitive equation model must be -3.

4. Results for a run with an annual cycle

Next, we integrated the same model for 100 years with the annual-cycle forcing as described in Section 2. Figure 3 illustrates the time series of the total energy of the model atmosphere for the first 10 and 100 years, respectively, for (a) and (b). Those time series are the plots of 10-day and 100-day means during 10 and 100 years, respectively as in the previous case. Figure 3a shows random variations of the energy level around the equilibrium state of about 15×10^5 Jm^{-2}. This time series contains low-frequency intraseasonal variabilities superimposed on the annual cycle. We find that the total energy oscillates within the range from 12 to 20 $\times$ 10^5 Jm^{-2}. The initial adjustment of the model atmosphere from an axisymmetric flow is seen at the left-edge of the time series. Figure 3b is for the 100-day mean time series during 100 years. Although the 100-day mean filters out most of the dominant oscillations, the annual cycle still remains clear, showing 100 sharp peaks in the time series. Both the intraseasonal and interannual variabilities are detectable in the time series. However, there is no clear trend nor systematic interdecadal variations as in the case of Section 3.

Figure 4 illustrates the power spectrum of the time series of the total energy for the 100-year integration with the annual cycle. The power spectrum is estimated by the same FFT routines as for the 1000-year daily data. Since the frequency resolution is 10 times coarser than the 1000-year run, the original power spectrum is averaged for every 8 terms over the frequency domain to obtain the smoothed spectrum. The frequency resolution of the spectrum is still fine enough to argue the detailed spectral properties. The result shows that the main difference between these two runs with and without the forced annual cycle is the sharp spectral peak at the one-year period detected in Fig. 4. The result clearly separates the two characteristic spectral slopes at the low- and high-frequency ranges. As in the previous case, the spectrum is white for a period beyond 50 days, and it is red for a period shorter than 50 days. The spectral slope indicates the same -3 power law. These features are identical to the former results shown in Fig. 2. It is important to note from the comparison of the results that there are no obvious harmonics nor subharmonics associated with the forced annual cycle. The semi-annual oscillation and biennial oscillation are most likely to be excited since these are the first harmonics and the subharmonics, respectively. We find, however, that the spectral peaks are missing, even for those oscillations.

The result of this study is compared with the conclusion derived by Zhao and Takahashi (1996) who have proposed conversely that the intraseasonal and interannual oscillations may be excitation as the result of the superharmonic and subharmonic resonances with the seasonal cycle, respectively. They considered the response of the tropical Kelvin waves to the cumulus heating with a seasonal cycle under a certain form of damping to derive so-called Mathieu equation in a form:

$$\frac{d^2U}{dt^2} = [a - 2q\cos(2t)]\,U. \tag{20}$$

The Mathieu equation is linear with respect to a state variable U and is represented by an inherent oscillation parameter a and an annual-cycle controller q. The equation may be regarded as a simple harmonic oscillator with an external annual forcing which is a product of U. The linear solution is known to have superharmonic and subharmonic resonances which is referred to as parametric instability. Compared with their model, our model is highly non-linear with a complete representation of advection. The superharmonic and subharmonic resonances may have occurred locally in our model, but the results appear to be highly turbulent, indicating a spectral power low at the all frequency bands. In this study the harmonics and subharmonics were expected as a result of the non-linear interactions of the internal dynamics of the strong annual cycle, rather than a modulation of the external forcing. The results suggest that the harmonics and subharmonics have been filled up by the white and red noise due to the vigorous turbulent mixing.

The result of this study is further compared with a laboratory experiment of a 2-D turbulence theory in Fig. 5 for developing harmonic resonances (see Sato, 1991). Figure 5a schematically illustrates an initial state of a forced line spectrum superimposed on a background noise (dashed line). Due to the non-

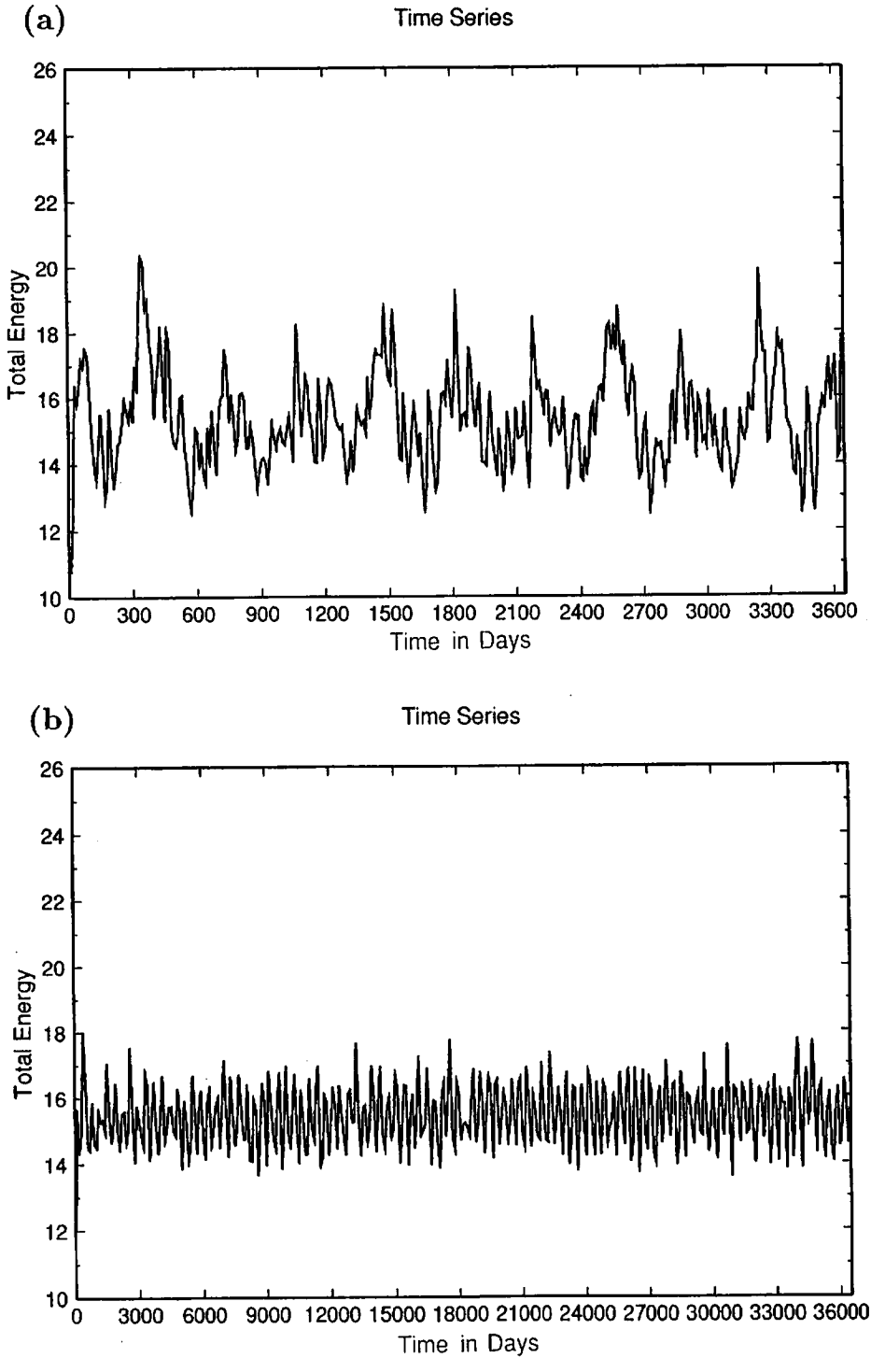

Fig. 3. As in Fig. 1, but for the experiment with the annual cycle forcing. The values in the figures contain 365 points of data for (a) 10-day mean during 10 years and (b) 100-day mean during 100 years, respectively. The units are 10^5 Jm^{-2}.

linearity of the fluid system, the forced line spectrum yields its harmonics as seen in Fig. 5b. The exited line spectra can interact with the continuous spectrum of the background noise to raise the energy level of the background noise, as in Fig. 5c. Finally, the energy of the fluid has spread over the all frequency ranges to reach to a saturated turbulent flow, as seen in Fig. 5d. The sequence of the pictures is quite instructive to understand the result of this study. Intuitively speaking, the harmonics and subharmonics might have been excited in our non-linear model by the inclusion of the forced annual cycle. However, the non-linear scattering of the energy peaks associated with these line spectra is so strong that the weaker spectral peaks seem to have spread away over the rest of the spectral range.

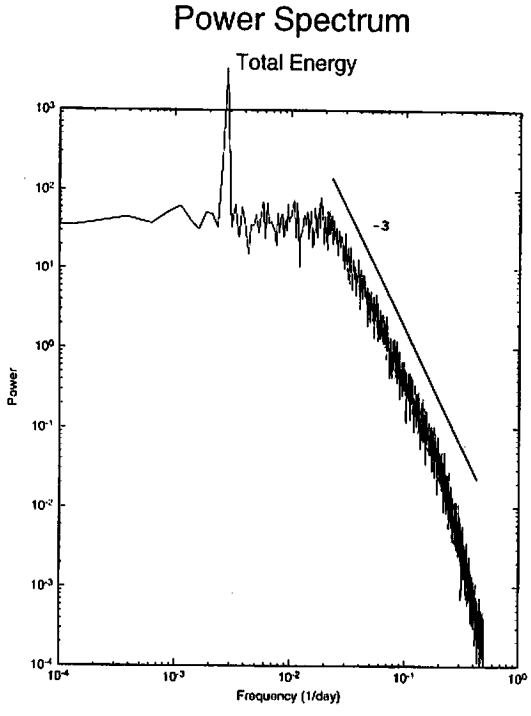

Fig. 4. As in Fig. 2, but for the experiment with the annual cycle forcing for the 100-year integration. The power spectrum is estimated by the FFT routines and is smoothed by averaging 8 terms of the original power spectrum. The sharp spectral peak corresponds to the annual cycle.

In other words, the atmosphere is highly turbulent, containing a saturated amount of energy over the all frequencies and to have obscured the harmonics and subharmonics.

5. Summary and concluding remarks

The first part of the objectives of this study is to find the typical magnitude and spectral features of natural variability of the model atmosphere by a long-term (1000 years) integration of a simple model under a fixed boundary condition. The results of the 1000-year time integration may be summarized as follows:

1. The time series of total energy of the model atmosphere shows the long-term average of 17 $\times$ 10^5 Jm^{-2} and the natural variability within the range of 14 $\sim$ 22 $\times$ 10^5 Jm^{-2}, indicating a clear intraseasonal variability with its period about 50 days.

2. The frequency spectrum of the model atmosphere is characterized as a white noise for the low-frequency variability with its period longer than 50 days. In contrast, the spectrum is characterized as a red noise for the period shorter than 50 days.

3. It is found from this study that the red-noise spectrum over the spectral range for $(50\text{-day})^{-1}$ to $(5\text{-day})^{-1}$ obeys a characteristic -3 power low. Since the sole energy source into the system is a parameterized baroclinic instability at a frequency of about $(5\text{-day})^{-1}$, we must have a reverse energy cascade from higher- to lower-frequency ranges along the -3 power slope of the red-noise spectrum.

Both the intraseasonal and interannual oscillations are detectable in the original time series as a part of the red and white noise. The result of the time spectral analysis indicates, however, no specific spectral peak associated with the intraseasonal time scale (about 50 days). The apparent intraseasonal variability may have resulted from the sharp transition from the red to white noise at a frequency of about $(50\text{ days})^{-1}$. The transition to white noise at the very-low-frequency range implies a reduction of the spectral power compared with the case of a red noise extending all the way to the very-low-frequency range. For this reason, the 50-day oscillation appears to be most dominant over the wide range of the frequency. This interpretation may be applied to some intraseasonal variabilities observed in the real atmosphere. Namely, an intraseasonal variability in the atmosphere may be regarded simply as the low-frequency edge of the red noise.

It is still unclear why the spectral features shift from red to white at the specific frequency about $(50\text{ days})^{-1}$. One of the possible interpretations of the question is to relate to the widely-known fact of the linear relation between life-time scale and spatial scale of prominent atmospheric phenomena, such as boundary-layer turbulence, cumulus convection, synoptic disturbances, and planetary waves. As far as the atmospheric phenomena lie on the universal line of the time-space relation, the time spectrum tends to be red since the larger is the spatial scale, the more is the spectral energy. Once the time scale exceeds about 50 days, the time-space relation breaks down due to the finite scale of the Earth. Then, the spectral energy of very-low-frequency variability can not sustain large energy, as expected from the extrapolation of the red-noise power spectrum. Therefore, the spectral energy level is bounded from above for the very-low-frequency variability to result in the white-noise spectrum. Although this interpretation is yet a speculation under the subject of further examination, we propose that the clear transition from the red to white noise is related to the finite size of the Earth.

The second part of the objectives of this study is to find whether the imposed annual-cycle forcing could generate its harmonics and subharmonics, such as semiannual and biennial oscillations, by means of the non-linear dynamic modulation of the

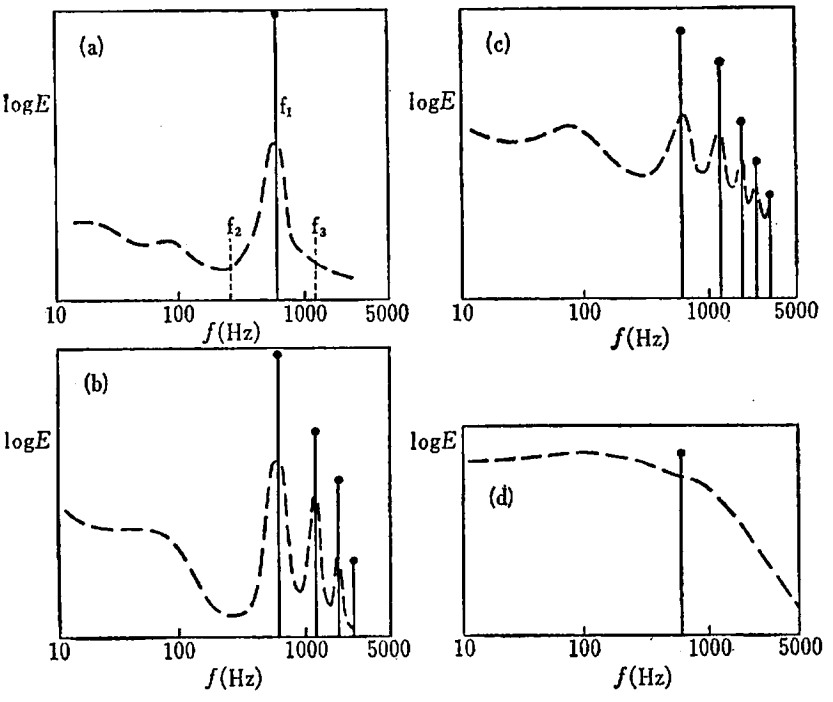

Fig. 5. Schematic illustration of develping harmonic resonances (line spectra), and a saturation of turbulent energy (dashed line) over the entire frequency range (after Sato, 1991). Refer to the text for the detail of the explanation.

strong annual cycle. The results of the 100-year time integration of the simple model with the forced annual cycle may be summarized as follows:

1. By changing the growth rate of the parameterized baroclinic instability over the 60–100 % range of the standard winter condition, we find that the total energy oscillates over the range from 12 to 20 $\times$ 10^5 Jm^{-2}. A clear spectral peak is generated at the one-year period, as expected.

2. The frequency spectrum is characterized as a white noise for the period beyond 50 days, and it is red for the period shorter than 50 days. These features are not altered by the inclusion and exclusion of the annual cycle.

3. The spectral peaks corresponding to the harmonics and subharmonics of the forced annual cycle, such as semiannual and biennial oscillations, are missing by the results of the spectral analysis.

According to the results, we may conclude that the semiannual and biennial oscillations are not excited by the internal non-linear modulation of the forced annual cycle as far as the total energy is concerned. Further studies may be necessary to understand the spectral features of the natural variability, especially for the cause of the clear separation of the red and white noises at the intermediate frequency range. A clear dynamical explanation is also desired for the -3 power law of the red-noise spectrum.

Acknowledgments

This research is jointly supported by the Grant-In-Aid from the Ministry of Education under the numbers 05452077 and 05NP0203. Partial support came from Arctic Region Supercomputing Center under an account ATMOS for the computation. The authors appreciate Ms. K. Honda for her technical assistance.

References

Dickinson, R.E., 1968: On the exact and approximate linear theory of vertical propagating planetary Rossby waves forced at a spherical lower boundary. *Mon. Wea. Rev.*, **96**, 405–415.

Hansen, J., I. Fung, A. Lacis, D. Rind, S. Lebedeff, R. Ruedy and G. Russell, 1988: Global climate changes as forecast by Goddard Institute for Space Studies three-dimensional model. *J. Geophys. Res.*, **93**, 9341–9364.

Hasselmann, K., 1976: Stochastic climate models. *Tellus*, **28**, 473–485.

James, I.N. and L.J. Gray, 1986: Concerning the effect of surface drag on the circulation of a baroclinic planetary atmosphere. *Quart. J. Roy. Meteor. Soc.*, **112**, 1231–1250.

James, I.N. and P.M. James, 1989: Ultra-low-frequency variability in a simple atmospheric circulation model. *Nature*, **342**, 53–55.

James, P.M., K. Fraedrich and I.N. James, 1994: Wave-zonal flow interaction and ultra-low-frequency variability. *Quart. J. Roy. Meteor. Soc.*, **120**, 1045–1067.

Kung, E.C., 1988: Spectral energetics of the general circulation and time spectra of transient waves during the FGGE year. *J. Climate*, **1**, 5–19.

Manabe, S., R.J. Stouffer, M.J. Spellman and K. Bryan, 1991: Transient response of a coupled ocean-atmosphere model to gradual changes of atmospheric CO_2. Part I: Annual mean response. *J. Climate*, **4**, 786–818.

Manabe, S. and R.J. Stouffer, 1996: Low-frequency variability of surface air temperature in a 1000-year integration of a coupled ocean-atmosphere model. *J. Climate*, **9**, 376–393.

Sato, H., 1991: *Turbulence*. One point Physics, No. 17, Kyoritsu Pub. 140pp (in Japanese).

Sperber, K.R. and T.N. Palmer, 1995: *Interannual tropical rainfall variability in general circulation model simulations associated with the atmospheric model intercomparison project*. PCMDI Report No. 28, 79pp.

Stouffer, R.J., S. Manabe and K. Bryan, 1989:Interhemispheric asymmetry in climate response to agradual increase of atmospheric CO_2. *Nature*, **342**, 660–662.

Stouffer, R.J., S. Manabe and K. Ya. Vinnikov, 1994: Model assessment of the role of natural variability in recent global warming. *Nature*, **364**, 634–636.

Tanaka, H.L., 1991: A numerical simulation of amplification of low-frequency planetary waves and blocking formations by the upscale energy cascade. *Mon. Wea. Rev.*, **119**, 2919–2935.

Tanaka, H.L., 1995: A life-cycle of nonlinear baroclinic waves represented by 3-D spectral model. *Tellus*, **47A**, 697–704.

Tanaka, H.L. and E.C. Kung, 1988: Normal mode energetics of the general circulation during the FGGE year. *J. Atmos. Sci.*, **45**, 3723–3736.

Tanaka, H.L. and E.C. Kung, 1989: A study of low-frequency unstable planetary waves in realistic zonal and zonally varying basic states. *Tellus*, **41A**, 179–199.

Tanaka, H.L. and S. Sun, 1990: A study of baroclinic energy source for large-scale atmospheric normal modes. *J. Atmos. Sci.*, **47**, 2674–2695.

Wigley, T.M.L. and S.C.B. Raper, 1990: Natural variability of the climate system and detection of the greenhouse effect. *Nature*, **344**, 324–327.

Zhao, N. and M. Takahashi, 1996: Super- and subharmonic responses of tropical Kelvin waves to the heating with a seasonal modulation. *J. Meteor. Soc. Japan.*, **74**, 115–123.

年周期を含む順圧モデル大気における自然変動のスペクトル解析

田中　博・木村和央[1]・安成哲三
(筑波大学地球科学系)

本研究では、モデル大気の自然変動の大きさや周波数応答特性を解析するために、簡単な順圧プリミティブ方程式モデルを長期間(1000年)積分し、その時系列のスペクトル解析を行なった。

年周期強制を除いた実験では、周期約50日以上の長周期変動のスペクトル分布は一様白色であり、年々変動や百年単位の顕著な長周期変動は検出されなかった。しかし、周期約50日の特徴的な季節内振動が時系列のうえで検出され、これ以下の周期帯では周波数の-3乗に従う明瞭なレッドノイズスペクトルに遷移することが解かった。季節内振動に伴うスペクトルピークは存在しないことから、レッドノイズが一様白色に遷移する周波数で見かけ上の季節内振動が卓越することを示した。モデル大気の唯一のエネルギー供給はパラメタライズされた傾圧不安定による周期約5日の周波数帯にあり、ここから低周波数帯に向かってエネルギーが逆カスケードを引き起こし、レッドノイズやホワイトノイズスペクトルを形成している。内部力学の非線形性が卓越する周期約50日以上の周波数帯のスペクトル分布はホワイトノイズとなり、一部の線形項が卓越し大気現象の時空間スケールに特徴的な線形関係が保たれる周波数帯ではそれがレッドノイズとなると考えられる。

年周期強制を導入した実験では、ホワイトノイズ内部に生じる年周期スペクトルピークが、モデルの内部力学の非線形性によりその高調波(低調波)応答を引き起こすかどうかが調べられた。実験結果のスペクトル解析によると、励起されたスペクトルピークは年周期強制によるものだけで、高調波(低調波)応答は生じなかった。この結果から、季節内振動や年々変動がもし卓越するラインスペクトルを持つとすれば、それらは外部強制として励起される必要があり、モデルの内部力学の非線形性による年周期変動の高調波(低調波)応答では生じないことが示された。

[1]現在浜銀総合研究所